Journal of Advanced Research xxx (xxxx) xxx

Contents lists available at ScienceDirect

Journal of Advanced Research

journal homepage: www.elsevier.com/locate/jare

Original Manuscript

Tetrahydroxy stilbene glucoside rejuvenates aging hematopoietic stem cells with predilection for lymphoid differentiation via AMPK and Tet2

Dan Gao [a,c,1], Wei-wei Yi [d,1], Bo Liu [d], Cong-en Zhang [e], Cui-cui Yang [a], Li Zeng [g], Lin Li [a], Guangbin Luo [f,h,*], Lan Zhang [a,*], Zhen-yu Ju [d,*], Jia-bo Wang [b,*]

[a] Department of Pharmacy, Xuanwu Hospital of Capital Medical University, National Clinical Research Center for Geriatric Diseases, Beijing Engineering Research Center for Nervous System Drugs, Beijing Institute for Brain Disorders, Key Laboratory for Neurodegenerative Diseases of Ministry of Education, Beijing 100053, China
[b] School of Chinese Medicine, Capital Medical University, Beijing 100069, China
[c] Key Laboratory of Endemic and Ethnic Diseases, Ministry of Education, Guizhou Medical University, Guiyang 550004, China
[d] Key Laboratory of Regenerative Medicine of Ministry of Education, Institute of Aging and Regenerative Medicine, Jinan University, Guangzhou, Guangdong 510632, China
[e] Department of Pharmacy, Beijing Friendship Hospital of Capital Medical University, Beijing 100050, China
[f] Department of Genetics and Genome Sciences, Case Western Reserve University School of Medicine, Cleveland, OH 44106-1712, USA
[g] Faculty of Chinese Medicine, Macau University of Science and Technology, Taipa, Macau, China
[h] Centre for Translational Medicine, Shenzhen Bao'an Chinese Medicine Hospital, Guangzhou University of Chinese Medicine, Shenzhen 518101, China

HIGHLIGHTS

- A set of nine selected agents were first tested for their effects on the premature aging of the hematopoietic system in total body irradiated (TBI) mice.
- 2,3,5,4′-tetrahydroxystilbene-2-O-β-D-glucoside (TSG) was successfully identified as a potent rejuvenating agent for aging HSCs.
- TSG treatment significantly increased the absolute number of common lymphoid progenitors (CLPs) along with their downstream B lymphocytes both in TBI mice and naturally aging mice.
- TSG treatment boosted the HSCs/CLPs repopulation potential of aging mice without causing any significant adverse effects.
- TSG supplementation restored the loss of regenerative capacity and decline in lymphopoiesis via AMPK-Tet2 axis.

GRAPHICAL ABSTRACT

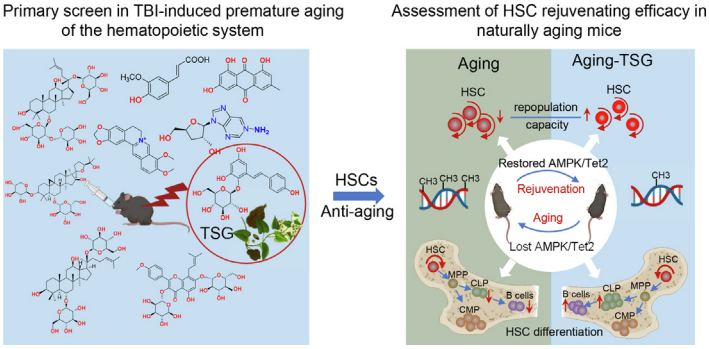

ARTICLE INFO

Article history:
Received 28 December 2023

ABSTRACT

* Corresponding authors at: School of Chinese Medicine, Capital Medical University, Beijing 100069, China (J.b. Wang); Key Laboratory of Regenerative Medicine of Ministry of Education, Institute of Aging and Regenerative Medicine, Jinan University, Guangzhou, Guangdong 510632, China (Z.y. Ju); Department of Pharmacy, Xuanwu Hospital of Capital Medical University, National Clinical Research Center for Geriatric Diseases, Beijing Engineering Research Center for Nervous System Drugs, Beijing Institute for Brain Disorders, Key Laboratory for Neurodegenerative Diseases of Ministry of Education, Beijing 100053, China (L. Zhang); Department of Genetics and Genome Sciences, Case Western Reserve University School of Medicine, Cleveland, OH 44106-1712, USA (G. Luo).
E-mail addresses: luol35@hotmail.com (G. Luo), lanizhg@126.com (L. Zhang), zhenyuju@163.com (Z.-y. Ju), jiabo_wang@ccmu.edu.cn (J.-b. Wang).
[1] Dan Gao and Wei-wei Yi contributed equally to this work.

https://doi.org/10.1016/j.jare.2024.04.027
2090-1232/

Please cite this article as: D. Gao, Wei-wei Yi, B. Liu et al., Tetrahydroxy stilbene glucoside rejuvenates aging hematopoietic stem cells with predilection for lymphoid differentiation via AMPK and Tet2, Journal of Advanced Research, https://doi.org/10.1016/j.jare.2024.04.027

Revised 26 March 2024
Accepted 26 April 2024
Available online xxxx

Keywords:
Tetrahydroxy stilbene glucoside
Aging
Hematopoietic stem cells
Lymphoid differentiation
AMPK-Tet2 axis

Introduction: Aging of hematopoietic stem cells (HSCs) has emerged as an important challenge to human health. Recent advances have raised the prospect of rejuvenating aging HSCs via specific medical interventions, including pharmacological treatments. Nonetheless, efforts to develop such drugs are still in infancy until now.
Objectives: We aimed to screen the prospective agents that can rejuvenate aging HSCs and explore the potential mechanisms.
Methods: We screened a set of natural anti-aging compounds through oral administration to sub-lethally irradiated mice, and identified 2,3,5,4′-tetrahydroxystilbene-2-O-β-D-glucoside (TSG) as a potent rejuvenating agent for aging HSCs. Then naturally aged mice were used for the follow-up assessment to determine the HSC rejuvenating potential of TSG. Finally, based on the transcriptome and DNA methylation analysis, we validated the role of the AMP-activated protein kinase (AMPK)-ten-eleven-translocation 2 (Tet2) axis (the AMPK-Tet2 axis) as the underlying mechanisms of TSG for ameliorating HSCs aging.
Results: TSG treatment not only significantly increased the absolute number of common lymphoid progenitors (CLPs) along with B lymphocytes, but also boosted the HSCs/CLPs repopulation potential of aging mice. Further elaborated mechanism research demonstrated that TSG supplementation restored the stemness of aging HSCs, as well as promoted an epigenetic reprograming that was associated with an improved regenerative capacity and an increased rate of lymphopoiesis. Such effects were diminished when the mice were co-treated with an AMPK inhibitor, or when it was performed in *Tet2* knockout mice as well as senescent cells assay.
Conclusion: TSG is effective in rejuvenating aging HSCs by modulating the AMPK- Tet2 axis and thus represents a potential candidate for developing effective HSC rejuvenating therapies.

Introduction

The human body possesses certain multipotent precursors in the form of hematopoietic stem cells (HSCs), found primarily in the bone marrow niche, which have the ability to self-renew, proliferate, and differentiate into myeloid and lymphoid progenitors, leading to the balanced production of both myeloid and lymphoid lineages to maintain the homeostasis of the blood lineage and the immune system of our body [1]. However, aging of the human body causes the HSCs to lose the ability of maintaining homeostasis of the hematopoietic system, resulting in the attenuated lymphopoiesis but myeloid-biased pattern of differentiation as well as the deterioration in repopulation capacity through HSCs transplantation[2,3] (for simplicity, such HSCs are referred to as "aging HSCs" herein). As the average human lifespan continues to extend, so does the proportion and the absolute number of individuals with advanced ages. Consequently, the loss of homeostasis and the diseases associated with the aging of the hematopoietic system pose a substantial challenge[4,5]. Recent animal studies have established that aging HSCs could be partially revitalized by opting for specific genetic or pharmacological intervention in mice, which serves as the proof-of-concept demonstrating the feasibility of rejuvenating aging HSCs[6,7]. This breakthrough offers the possibility of rejuvenating aging humans HSCs through specific medical interventions, such as pharmacological drug treatments. Nonetheless, efforts to develop such drugs are still in their infancy to date.

Currently, several compounds including rapamycin, CASIN, TN13, SB203580 and ABT263[6], have been reported to possess certain capacities of rejuvenating aging HSCs under various experimental settings. However, the task of getting any of them to be approved as an HSC rejuvenating drug would likely still prove costly and time consuming. Meanwhile, it has been recognized that certain formulas of traditional Chinese medicine (TCM) have been claimed to possess the property of rejuvenating aging HSCs and safe for human uses even over a long period of time. While the efficacy aspects of such claims are usually not based on unbiased randomized clinical trial experiments, the safety aspects are general accepted when they are used according to the specific guidelines. Thus, if the efficacy issue would be validated, the paths to a successful clinical development for such medicine would be much more desirable. The proof of the clinical efficacy of a TCM, on the one hand, would greatly encourage the effort to conduct the proper randomized clinical trials to improve its quality and use in the form of TCM; while on the other hand, could significantly minimize the concern of the risk issue of modern drug development should a compound-based modern drug development path be chosen.

In this study, we screened a set of presumed natural anti-aging compounds derived from several well-known TCM formulas and identified 2,3,5,4′-tetrahydroxystilbene-2-O-β-D-glucoside (TSG) as a powerful rejuvenator for aging HSCs. The corresponding mouse equivalent dose for each compound was derived from the human dose in accordance with the recognized safety requirements and the well-regarded effectiveness for the parent TCM ingredient. TSG is a natural derivative of polyphenols from the TCM "Heshouwu", that had been well known for a multitude beneficial effects including anti-oxidation[8], anti-inflammation[9], anti-hyperlipidaemia[10] and neuroprotection[11,12] as well as anti-aging. In this study, we found that TSG treatment not only greatly raised the absolute quantity of common lymphoid progenitors (CLPs) along with their downstream B lymphocytes, but also enhanced the ability for the HSCs/CLPs repopulation through the rapid expansion in donor chimerism of aging mice. Furthermore, TSG could restore the quiescence of aging HSCs and promote the epigenetic reprogramming that exhibited to alter DNA methylation profile for the control of HSC fate decisions by activating the AMP-activated protein kinase (AMPK) and its substrate Ten-eleven-translocation 2 (Tet2). This study opened an avenue to mitigate HSCs aging by activating AMPK and positively identified TSG as a very promising candidate acting as a natural AMPK activator for developing anti-aging drugs for rejuvenating aging HSCs in humans.

Materials and methods

Mice

"Young" (approximately 8-week-old) wild-type C57BL/6J mice (CD45.2) of both genders were acquired from Sipeifu Biotechnology Co., Ltd. (Beijing, China), while "aging mice" (approximately 80-week-old) mice were bred and aged in-house. The recipient mice used in the transplantation assays were either CD45.1 or

CD45.1/CD45.2 mice (C57BL/6J congenic strain of mice). The *Tet2* mutant mice (*Tet2*$^{m/m}$, herein after termed as *Tet2* Mut) was a generous gift from Drs. Shaorong Gao and Jiayu Chen of Tongji University. Details about generation of *Tet2* catalytic mutant mouse are described in the supplementary materials. The mice were housed under a 12-hour light–dark cycle, with unrestricted access to food and water. For our studies, we employed mice of both sexes, without employing any particular randomization or blinding approaches in the selection process.

Mouse models and treatments

To screen a library of natural anti-aging compounds on radiation induced premature aging of the hematopoietic system, 8-week-old C57BL/6J mice were subjected to either sham irradiation as controls or a sublethal 4 Gy dose of X-ray radiation (RS2000XE, Rad Source) for total body irradiation (TBI), with a dose rate of 0.4 Gy/min. After TBI treatment, the mice were treated with either vehicle (saline) or compound solutions. All following compounds were administered at the various doses (mg per kg body weight per day (mg/kg/d)) as the following: astragaloside Ⅳ at 50 mg/kg/d, berberine at 100 mg/kg/d, cordycepin at 100 mg/kg/d, emodin at 30 mg/kg/d, ferulic acid at 100 mg/kg/d, ginsenoside Rg1 at 60 mg/kg/d, icariin at 50 mg/kg/d, notoginsenoside R1 at 30 mg/kg/d, and tetrahydroxy stilbene glucoside (TSG) at 120 mg/kg/d were administered to the TBI mice by gavage for 60 days, respectively. Subsequently, aging C57BL/6J mice received TSG orally at a dosage of 120 mg/kg/day for 60 days, while 5-aminoimidazole-4-carboxamide riboside (AICAR, absin, abs812834, China) was administered intraperitoneally at a dose of 50 mg/kg daily for the same period. The administration of compound C (Com C, Selleck, S7306, USA) at 10 mg/kg intraperitoneally every alternate day was followed by TSG oral dosing. 40-week-old *Tet2* Mut mice displayed a more evident CLP decrease and skewed myeloid/lymphoid ratio than 16 weeks of age[13]. *Tet2* Mut mice at 40-week-old were treated with vehicle (saline) or TSG solution by gavage for 60 days, respectively. All natural compounds were sourced from Chengdu Pufei De Biotech Co., Ltd., China. Each experiment consisted of 4 mice per group, and mice were sacrificed to analyze as described below. All experiments were replicated a minimum of three times.

FACS analyses

Immunostaining of preparations of bone marrow (BM), thymus, and peripheral blood (PB) were performed according to standard protocols and analyzed with LSRII/Fortessa (BD Biosciences, USA) or sorted by Influx (BD Biosciences, USA). BM cells were harvested by mechanically disrupting leg, pelvic bones, and spines in a staining medium, specifically phosphate-buffered saline (PBS, Sigma, USA) enriched with 0.2 % bovine serum albumin (BSA, Sigma, USA). Individual thymus was isolated and disintegrated through 45-μm cell strainers (Corning BD Falcon, USA) in PBS to yield single-cell suspensions. Each PB sample was collected from the orbital vein into a EDTA (0.1 M)-containing tube. Erythrocytes were removed by red blood cell lysis buffer (BD Biosciences, USA). For hematopoietic stem/progenitor cells analysis, BM cells were stained with biotinylated anti-mouse cocktail antibodies specific for the following lineage (Lin) markers (Biolegend, USA): CD4 (RM4-5), CD8 (53–6.7), B220 (RA3-6B2), CD11b (M1/70), TER-119, and Gr-1 (RB6-8C5) to label lineage-negative (Lin-) cells and then stained with c-Kit (ACK2, eBioscience, USA), Sca-1 (El3-161.7, Biolegend, USA), streptavidin (BD Biosciences, USA), CD48 (HM48-1, Biolegend, USA), CD150 (TC15-12F12.2, Biolegend, USA), CD34 (RAM34, BD Biosciences, USA), Flk2 (A2F10, BD Biosciences, USA), IL-7R (A7R34, BD Biosciences, USA), and CD16/32 (93, BD Biosciences, USA). For B, T, and myeloid cells analyses, BM cells were stained with CD4 (RM4-5, Biolegend, USA), CD8 (53–6.7, Biolegend, USA), B220 (RA3-6B2, Biolegend, USA), CD43 (eBioR2/60, eBioscience, USA), CD19 (eBio1D3, eBioscience, USA), IgM (11/41, Biolegend, USA), and CD11b (M1/70, BD, USA); PB and spleen cells were stained with CD4 (RM4-5, Biolegend, USA), CD8 (53–6.7, Biolegend, USA), B220 (RA3-6B2, Biolegend, USA), and CD11b (M1/70, BD, USA). For thymic T cell analyses, cells were stained with CD4 and CD8. Enrichment of c-Kit$^+$ cells was achieved using anti-APC c-Kit microbeads (Miltenyi Biotec, Germany) and MACS Separation LS Columns (Miltenyi Biotec, Germany), with LTs sorted on BD Influx (Becton Dickson, USA) post-staining with c-Kit, Sca-1, streptavidin, CD34, and Flk2. For BM and PB donor-derived chimerism analyses, cells were stained with conventional label scheme together with CD45.1 (A20, Biolegend, USA) and CD45.2 (104, eBioscience, USA). Stained cells were re-suspended in staining media with 1 μg/ml 4′,6-diamidino-2-phenylindole (DAPI, Sigma-Aldrich, USA) to exclude dead cells. Intracellular staining involved initial antibody application, followed by anti-Ki67 (eBioscience, 11–5698-80, USA) staining in perm/wash for 40 min at room temperature, shielded from light. After a wash in perm/wash, cells were suspended in PBS with 1 μg/ml DAPI for a 20-minute incubation followed by fluorescence-activated cell sorting (FACS) analysis. Data analysis was conducted using the FlowJo software.

Bone marrow transplantation

Competitive transplantation experiments were performed by transplanting 500 LTs purified from donor mice (C57BL/6J CD45.2) together with total BM cells (5×10^5) from young (2–4-month-old) competitor mice (CD45.1) into lethally irradiated (8 Gy) recipients (CD45.1/CD45.2). Transplanted mice were fed antibiotic-containing water for 2 weeks, and the degrees of donor-derived chimerism were evaluated one a month by a FACS-based analysis of blood from *retro*-orbital bleeding. After 12 weeks of transplantations, recipients were sacrificed to measure the donor-derived contribution in the PB and BM. For non-competitive repopulation assays, 10^3 CLPs were immediately transplanted intravenously into irradiated (4 Gy) congenic C57BL/6J Ly5.1 mice. Three weeks after transplantation, donor cell contributions to the PB and BM of recipient mice were analyzed. Inhalation of ether for anesthesia was used when transplantation experiments were performed.

Ethics statement

Experimental procedures involving animals received approval from the Animal Welfare and Ethics Committee of the Fifth Medical Centre of the Chinese PLA (People's Liberation Army) General Hospital, and were conducted adhering to the established ethical guidelines, with the ethical approval number IACUC-2020-0048.

Cell culture

IMR-90 fibroblasts (catalog number CCL-186) were initially procured from the American Type Culture Collection in Manassas, VA, USA. These cells were cultured in Dulbecco's Modified Eagle Medium, with 10 % fetal bovine serum (FBS), 100 U/ml penicillin, and 100 μg/ml streptomycin (all reagents sourced from Gibco, USA). The culturing environment was a humidified incubator, maintained at 37 °C with a 5 % CO_2 atmosphere. The IMR-90 fibroblasts, after surpassing 25 passages, entered a phase of replicative senescence. To promote this senescence, the cells were subcultured regularly until a marked reduction in division rate was observed, typically around the 40th passage. IMR-90 cells at 60–70 % conflu-

ency and at the 40th passage were treated with varying concentrations of tetrahydroxy stilbene glucoside (TSG, 10 and 100 μM) for 48 h. In some instances, these cells were also exposed to the AMPK inhibitor Compound C (Com C, 10 μM, Selleck, USA) in combination with TSG, or to the AMPK activator AICAR (0.5 mM, absin, China) for the same duration. After the treatments, the cells were harvested for protein analysis via western blotting.

Western blot analysis

Cell lysis was performed using RIPA buffer, followed by the determination of protein concentrations via the bicinchoninic acid (BCA) assay. The proteins were then separated using 8–16 % SDS-PAGE gels supplied by Genscript (catalog number M81612). After the electrophoresis, the proteins were transferred onto PVDF membranes (Millipore). These membranes were subsequently blocked with 5 % bovine serum albumin (BSA) in Tris-buffered saline with 0.1 % Tween (TBST) at room temperature for 60 min, followed by an overnight incubation with primary antibodies at 4 °C. This step was followed by triple washing with TBST and a subsequent 1-hour incubation at 4 °C with the corresponding secondary antibodies. Detection was performed using the Odyssey Infrared Imaging System from Bio-Rad. The primary antibodies utilized were rabbit anti-AMPKα (Cell Signaling Technology, 2532, USA), rabbit anti-phospho-AMPKα (Cell Signaling Technology, Thr172, 2535, USA), rabbit anti-phospho-acetyl-CoA carboxylase (Cell Signaling Technology, Ser79, 3661, USA), rabbit anti-Tet2 (bioworld, BS7804, China), and mouse anti-β-actin (Sigma, A1978, USA). For the secondary antibodies, IRDye 800CW Goat Anti-Rabbit IgG (Li-COR Biosciences, 926–32211, USA) and IRDye 800CW Goat Anti-Mouse IgG (Li-COR Biosciences, 926–32210, USA) were employed.

Seahorse metabolic flux experiments

Oxygen consumption rate (OCR) was measured by an XF96 extracellular flux analyzer (Seahorse Biosciences) adopting XF Cell Mito Stress Test kit according to the manufacturer's instructions (Agilent Technologies). In brief, sorted Lineage$^-$ Sca-1$^+$ c-Kit$^+$ (LSK) cells were adjusted to a concentration of 10^5 cells/well with 180 μl pre-adjusted + cyt media into XF cell culture microplate precoated for 3 h with poly-lysine (Sigma-Aldrich, P4707, USA) in 37 °C CO_2-free incubator. Compounds were then loaded into the appropriate ports of a hydrated sensor cartridge: The corresponding order of compounds oligomycin (1 μM), FCCP (2 μM), and rotenone/antimycin A (0.5 μM) were port A, port B, and port C, respectively. Mitochondrial ATP production was calculated based on the OCR differences upon addition of oligomycin from basal rate.

Quantitative real-time PCR analysis

Total RNA from LSK cells was isolated utilizing the RNeasy Mini Kit (Qiagen Germany). The synthesis of complementary DNA (cDNA) was then conducted using the PrimeScript™ RT reagent Kit (TAKARA, Japan). Quantitative PCR (qPCR) analyses were carried out employing SYBR Premix Ex Taq™ (TAKARA, Japan) on a CFX96 Real-Time System (Bio-Rad, USA). Details of the mouse-specific primers utilized in the qPCR can be found in Supplementary Table S1.

Molecular docking prediction

The crystallographic structures of AMPK(α1β1γ1) and AMPK (α2β1γ1) were retrieved from the RCSB Protein Data Bank, bearing the PDB codes 6C9F and 6B1U, respectively. These structures were then prepared as receptor models, using PyMol software to excise the original ligands and water molecules. For the small-molecule ligand, the two-dimensional structure of TSG was acquired from the TCMSP database (accessible at https://old.tcmsp-e.com/tcmsp.php) and saved in MOL2 file format. Subsequently, the 3D crystal structures of both protein targets and the TSG ligand were imported into the AutoDock 4.0 software for the purpose of conducting molecular docking studies.

Surface plasmon resonance (SPR) analysis

The binding interactions between Tetrahydroxy stilbene glucoside (TSG) and the AMPK isoforms α1β1γ1 and α2β1γ1 were examined using surface plasmon resonance (SPR) spectroscopy, utilizing a Biacore T200 biosensor device from GE Healthcare. For these analyses, each target protein was immobilized on a CM5 chip via an amine-coupling procedure. The binding experiments were conducted at a controlled temperature of 25℃ and a flow rate set at 30 μl/min. Various concentrations of the compounds (ranging from 0.78 to 50 μM) were prepared in a running buffer composed of 40 mM Tris, 150 mM NaCl, 0.2 mM CaCl2, 20 mM MgCl2, and Surfactant P20 (pH 7.4). These were then passed over the immobilized targets at the indicated gradient concentrations. The kinetic dissociation constant (KD) for each interaction was determined using the Biacore T200 evaluation software version 2.0 provided by GE Healthcare.

AMPK kinase activity assay

The ADP-Glo™ Kinase Assay (Promega, USA), a luminescent assay for measuring kinase activity, was employed to assess the activity of AMPK(α1β1γ1) and AMPK(α2β1γ1). This assay quantifies ADP produced in a kinase reaction, where ADP is subsequently converted to ATP, and then to light by Ultra-Glo™ Luciferase. The luminescence is directly proportional to the ADP quantity and kinase activity. According to the ADP-Glo™ Kinase Assay instructions, AMPK was exposed to various concentrations of tetrahydroxy stilbene glucoside (TSG) (ranging from 0 to 1 μM), with AMP serving as a positive control. Components including the enzyme, substrate, ATP, and inhibitors were diluted in Kinase Buffer. Within white, low-volume 384-well polystyrene plates, the reaction setup included 1 μl of inhibitor, 2 μl of enzyme, and 2 μl of substrate/ATP mixture. TSG and AMPK kinase solutions were also added. Control wells contained kinase buffer, substrate, and ATP but lacked the enzyme. These plates were incubated at room temperature for 60 min, followed by the addition of 5 μl of ADP-Glo reagent, and a further incubation for 40 min. Subsequently, 10 μl of Kinase Detection Reagent was added, and the plates were incubated for another 30 min at room temperature. Optical density (OD) readings were then obtained using a GloMax® Discover Multimode Microplate Reader (Promega Inc., USA). All experiments were conducted in triplicate.

RNA sequencing

RNA extraction was carried out from approximately 20,000 long-term hematopoietic stem cells (LTs) that were sorted using fluorescence-activated cell sorting (FACS) and purified using the RNeasy Micro Kit (QIAGEN Germany). The RNA sequencing (RNA-Seq) service was performed by Novogene Co., Ltd.(Beijing, China). Libraries for sequencing were constructed employing the NEBNext® Ultra™ RNA Library Prep Kit (Illumina, USA). Sequencing was executed on an Illumina Novaseq platform, generating 150 bp paired-end reads. Analysis of differentially expressed genes was conducted using the DESeq2 package (version 1.16.1) in R, setting a significance threshold at an adjusted P-value of < 0.05 and a fold-change of ≥ 2. The Cluster Profiler package was utilized for Gene Ontology (GO) enrichment and Kyoto Encyclopedia of Genes and Genomes (KEGG)

pathway analysis. Furthermore, Gene Set Enrichment Analysis (GSEA) (available at https://www.broadinstitute.org/gsea/index.jsp) was applied to pinpoint lymphoid-related gene sets in both young and aged mice, and in aged mice treated with vehicle or TSG. Gene sets pertaining to lymphopoiesis, hematopoietic stem cell metabolism, and cell cycle were considered significantly enriched at a P-value < 0.05 and a false discovery rate (FDR) < 0.25. The RNAseq data have been deposited in the Sequence Read Archive (SRA) database under the accession number PRJNA827524.

DNA methylation analysis

For each DNA preparation, DNA was extracted 1×10^5 to 4×10^5 cells from the bone marrow (BM) using the DNeasy Blood & Tissue Kit (Qiagen Germany). The preparation of reduced representation bisulfite sequencing (RRBS) libraries from a limited quantity of LTs involved the adaptation and refinement of a single-tube method. This approach notably decreased the number of PCR cycles necessary for library amplification, thereby preserving the integrity of the results, in line with previously established methods. Typically, a13 cycle-PCR of approximately 10 ng of genomic DNA was used to obtain sufficient DNA for the further analysis. After the PCR amplification, DNA fragments of 150 to 500 bp were harvested using SPRI select beads from Beckman Coulter and used to construct a library as described. For sequencing, the RRBS libraries were combined with either 20 % PhiX Control from Illumina or other balanced libraries, and pair-end 150 bp sequencing was conducted using the HiSeq 2500 sequencer (Illumina). The alignment of RRBS sequencing reads to the bisulfite-converted mouse genome (mm10) was executed with Bismark v0.10.1 (Babraham Bioinformatics). DNA methylation analysis was carried out as described previously[14].

Co-culture experiments

OP9 cells were maintained in α-MEM with 20 % fetal bovine serum (FBS), 40 μM 2-mercaptoethanol, and 2 mM L-glutamine. For the induction of lymphoid differentiation, LSK cells from the bone marrow of 8-week-old mice were co-cultured with 80 % confluent OP9 cells. The culture medium was α-MEM with 20 ng/ml Flt3 ligand (Flt3L), 10 ng/ml interleukin-7 (IL-7), and 100 ng/ml stem cell factor (SCF) (R&D Systems). For some experiments, TSG (10 and 100 μM) or the Tet2 inhibitor Bobcat339 (1 and 10 μM) were incorporated for around 72 h (determined by preliminary experiments). Subsequently, cells were labeled with anti-CD19 and anti-B220 antibodies for flow cytometry analysis.

Statistical analysis

Data sets were characterized by normal variance. Statistical results are presented as the mean ± standard deviation (S.D.). The statistical analyses were conducted using the SPSS 13.0 software (SPSS Inc., Chicago, IL, USA). For datasets involving multiple groups, either one-way ANOVA or two-way ANOVA, supplemented by a Tukey Kramer post hoc test, were employed to determine the p-values. The outcomes are expressed as mean ± SD. The symbols 'ns' denotes non-significance, whereas asterisks indicate levels of significance: $^{*}p < 0.05$; $^{**}p < 0.01$; $^{***}p < 0.001$.

Results

Screening for compounds capable of rejuvenating aging HSCs

It has been previously reported that total body irradiated (TBI) 8-week-old mice possessed premature aging of the hematopoietic system having key features reminiscent of those in naturally aging mice[15,16]. Since such TBI mice can be readily generated, we posited that they could be adopted as a model for the initial assessment on the potential of individual agents for rejuvenating aging HSCs. Such a model could then be used in conjunction with a follow-up confirmation test in the naturally aging mice as a system for identifying agents that possess the property of rejuvenating aging HSCs (Fig. 1a). Here, we chose to screen a unique library with a small number of hand-picked compounds that are known to exhibit highly conducive effects on hematopoiesis in humans. First, we conducted a preliminary experiment identified 9 candidate compounds derived from 9 different TCM formulas and established the proper equivalent oral dose for mice for each of them based on the corresponding dose that was recommended for humans (Table S2). When these compounds were subsequently screened under the TBI model system evaluated by the homeostasis of the hematopoietic system in the bone marrow (BM) using FACS analysis, one compound, 2,3,5,4′-tetrahydroxystilbene-2-O-β-D-glucoside (TSG), stood out by its potent capability of increasing the number of CLPs per mouse and the total number of both total B and pre-B cells in the TBI mice without any significant impact on the quantity of hematopoietic stem progenitor cells (HSPCs) and myeloid cells (data not shown) (Fig. 1b-e). Furthermore, TSG treatment significantly enhanced the TBI-induced drastic decrease of lymphoid lineages in the bone marrow, thymus, and the peripheral blood without any major adverse effects on the various components of the hematopoietic system including long-term hematopoietic stem cells (LTs), short-term hematopoietic stem cells (STs), common myeloid progenitors (CMPs), granulocyte/macrophage progenitors (GMPs) and megakaryocyte/erythroid progenitors (MEPs) in the bone marrow (Fig. S1a-g). Considering these data, TSG was identified as the first "hit" from the primary screen.

TSG exhibited a potent potential in rejuvenating aging HSCs without any significant adverse effects

The identification of TSG as the first "hit" from the primary screen then prompted us to further assess whether it could also rejuvenate aging HSCs in naturally aging mice. Hematopoietic stem cells (HSCs) can produce all known hematopoietic lineages and undergo self-renewal, accompanied by debilitations of lymphopoiesis during aging due to the decline in the capability of HSCs[5]. Studies showed that HSCs in mice of 80 weeks and older exhibit considerable aging characteristics, making such 80-week-old mice as an excellent model for studying the reversibility of HSC aging[17]. Thus, to examine the potential of TSG in rejuvenating aging HSCs, we administered TSG or the vehicle to cohorts of naturally aging mice for 60 days, and then evaluated the homeostasis of the hematopoietic system in the bone marrow. The results showed that mice treated with TSG had a significantly higher number of common lymphoid progenitors (CLPs, $Flk2^{+}IL\text{-}7R^{+}linage^{-}c\text{-}kit^{mid}Sca1^{mid}$) in the bone marrow per mouse (Fig. 2a), and also much higher numbers of total, pro-, and pre-B cells of the B lineage (Fig. 2b). Additionally, the TSG treatment on the naturally aging mice did not produce any substantial effects on the numbers of T and myeloid cells of the bone marrow (Fig. 2c). Nonetheless, it did result in significant elevations in the total numbers of three main sub-types of T cells including $CD4^{+}$-$CD8^{+}$ T cells and single-positive $CD4^{+}$ or $CD8^{+}$ T cells of the thymus (Fig. 2d). Moreover, compared to the untreated control, the TSG-treated mice also exhibited a significant higher percentage of B cells and a significant lower percentage of myeloid cells, but similar compositions of T cells in the peripheral blood (Fig. 2e).

Intriguingly, FACS analyses revealed that the absolute number of long-term hematopoietic stem cells (LTs, $CD150^{+}CD48^{-}linage^{-}c\text{-}kit^{+}Sca1^{+}$) and short-term hematopoietic stem cells (STs,

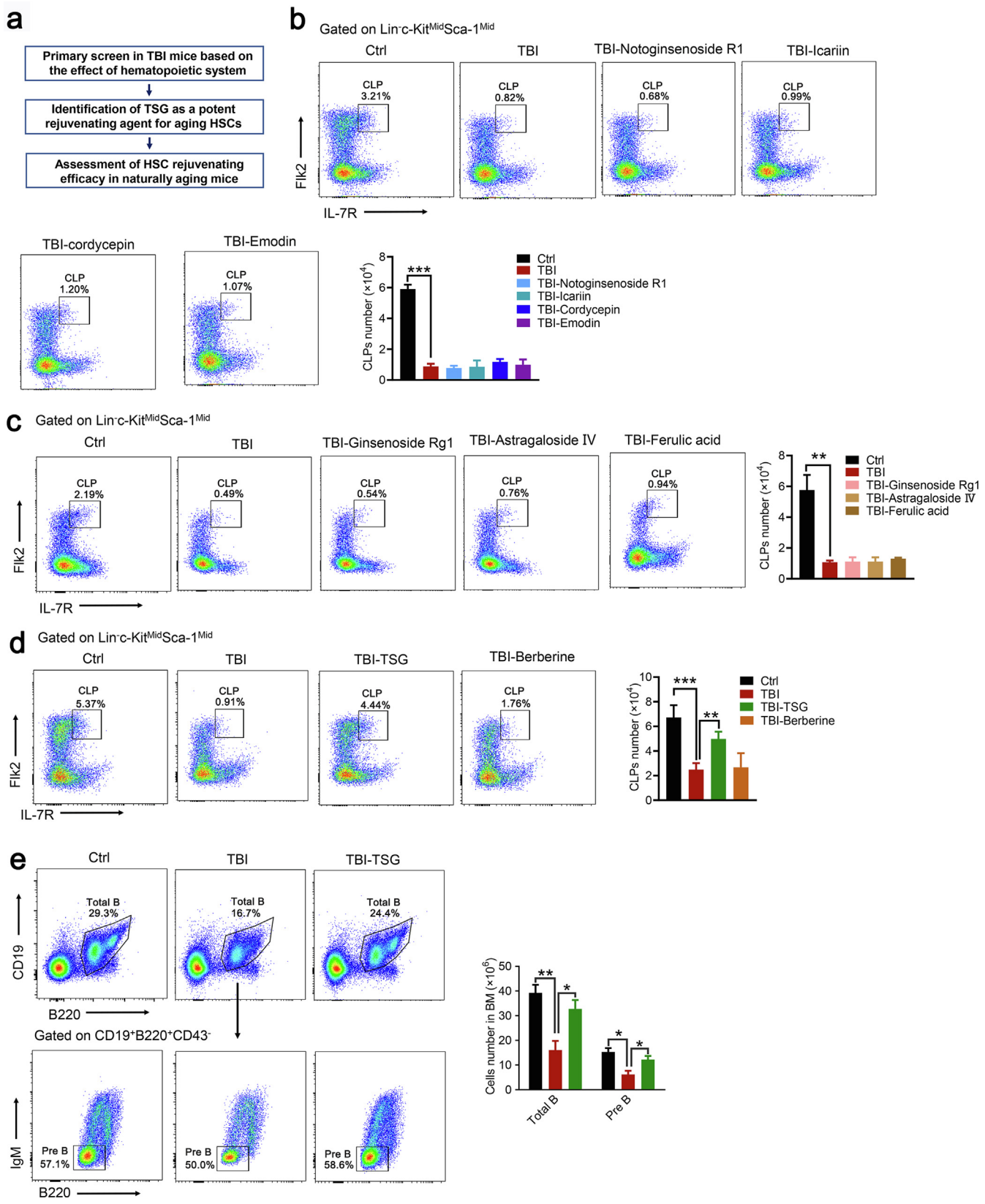

Fig. 1. A approach for screening agents with hematopoietic stem cell (HSC) rejuvenation potential. (a) A schematic illustration of the screening process. (b-d) A small number of candidate compounds are first hand-picked from highly acclaimed TCM antiaging herbs for hematopoiesis and the mice dosages are calculated based on the human dose. The primary experimental screen of nine selected agents is then first carried out with total body irradiated (TBI) mice to identify agents that have a significant positive effect on the systematic analysis of the hematopoietic system. When a positive agent is identified, it is then subjected to a secondary experimental screen in naturally aging mice based on the same criteria. When an agent passes this secondary screen, it is then subjected to a series of analyses for a full assessment of its efficacy in HSC rejuvenation in naturally aging mice. (d) Tetrahydroxy stilbene glucoside (TSG), the sole agent that was found to significantly improve the number of CLPs based on this test. (e) Specifically, the representative FACS plots and quantification of the total number of B cells and pre-B cells in the bone marrow (BM) of the untreated normal 8-week-old mice (Ctrl), TBI mice treated with vehicle (TBI), and TBI mice treated with tetrahydroxy stilbene glucoside (TBI-TSG) are shown. Data is presented as mean ± S.D. (n = 4). *: $p < 0.05$; **: $p < 0.01$; ***: $p < 0.001$.

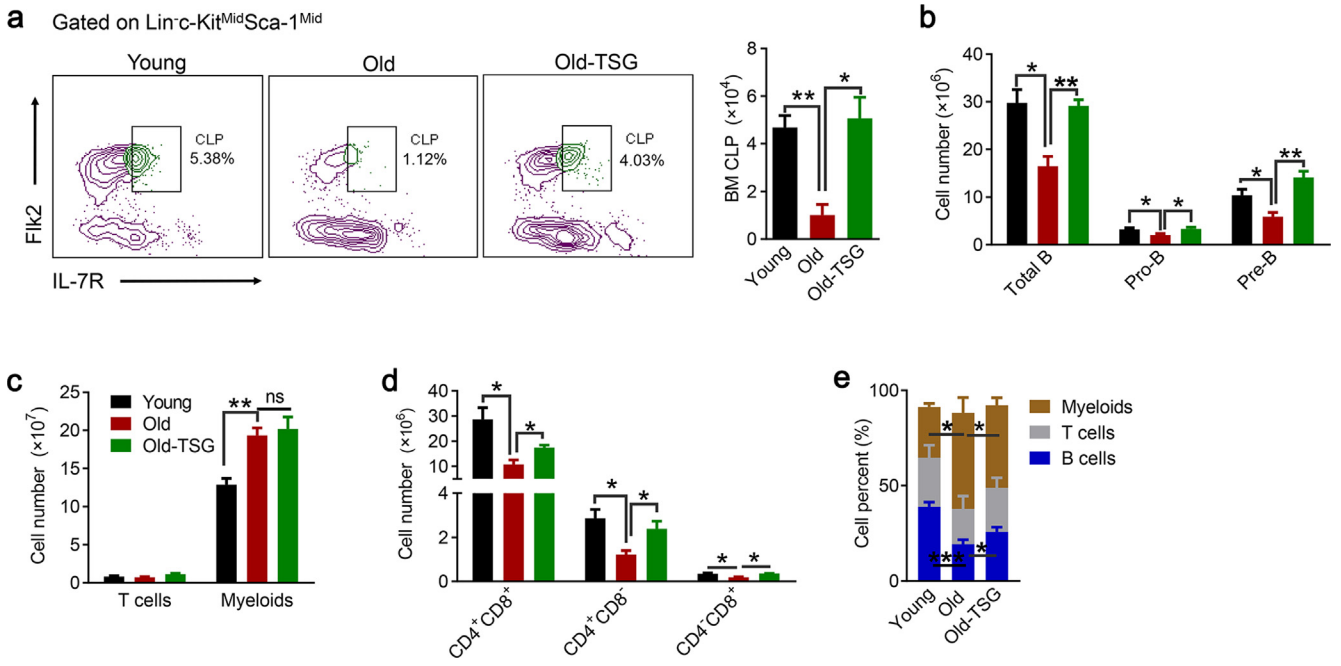

Fig. 2. Effects of tetrahydroxy stilbene glucoside (TSG) on key attributes of HSCs of naturally aging (80-week-old) mice. Cohorts of aging mice were treated with either vehicle (Old) or TSG (Old-TSG) for 60 days and analyzed. A cohort of 8-week-old mice was included as a control for young mice (Young). (a) Analysis of common lymphoid progenitors (CLPs). Representative FACS plots (The left panel) and quantification of CLPs (the right panel) from the bone marrow of different cohorts. (b) Absolute numbers of various sub-types of B cells in the bone marrow of different cohorts. (c) Absolute numbers of T and myeloid cells in the bone marrow of different cohorts. (d) Absolute numbers of different sub-types of T cells per thymus of different cohorts. (e) Mean percentages of peripheral B, T, and myeloid cells of different cohorts. Throughout, data is represented by mean ± S.D. (n = 4). *: $p < 0.05$; **: $p < 0.01$; ns: no significance.

$CD150^{-}CD48^{-}linage^{-}c\text{-}kit^{+}Sca1^{+}$) were increased 4–5 folds in the naturally aging mice as compared to the young mice. The TSG treatment did not cause any significant changes on the naturally aging mice (Fig. S2a). Besides, the TSG treatment did not produce any significant changes in the number of common myeloid progenitors (CMPs) and granulocyte/macrophage progenitors (GMPs), as well as the decreased number of megakaryocyte/erythroid progenitors (MEPs) in the bone marrow of naturally aging mice as compared to the young mice (Fig. S2b). Moreover, the TSG treatment did not alter the body weight, peripheral blood cells, blood chemistry, and the histological features of the liver in any prominent manners (Fig. S2 c-g). Hence, TSG was quite effective in rejuvenating aging HSCs, including being very effective in promoting the lymphopoiesis potential of aging HSCs without causing any significant adverse effects.

TSG can enhance the repopulation potential of aging HSCs

Aging HSCs are also known to exhibit a drastically reduced repopulation potential[18]. Thus, we then examined whether TSG could boost the repopulation capability of HSCs in aging mice. Firstly, we conducted the competitive bone marrow transplantation experiment by transplanting 500 LT-HSCs from donors of the young mice (8-week-old), the control aging mice (80-week-old), and the aging mice that were treated with TSG for 60 days, with half a million bone marrow cells from the competitor C57BL/6J CD45.1 mice into individual recipients radiated by lethal dose X-ray (C57BL/6J CD45.1/CD45.2 mice) and then examining their repopulation potentials (Fig. 3a). The results showed that the transplantation with the LT-HSCs with long-term multi-lineage potential from the young and the aging mice led to the highest and the lowest percentages of donor cell contribution for the peripheral blood cells (Fig. 3b) as well as for three different types of stem/progenitor cells (LSKs, HPCs, and LT-HSCs, respectively) in the bone marrow (Fig. 3c). Comparatively, the mice that received the LT-HSCs from the TSG-treated aging mice exhibited higher contributions in all the cases (Fig. 3b, c).

A CLP transplantation experiment was also performed by transplanting 10^3 CLPs obtained from the young mice, the control aging mice, and the aging mice that were treated with TSG for 60 days, intravenously into irradiated recipient mice (C57BL/6J CD45.1 mice) followed by assessing the donor cell contributions to the peripheral blood and to the bone marrow of the recipient mice at three weeks post transplantation (Fig. 3d). It was found that transplanting CLPs from the control aging mice resulted in remarkably lower percentages of total donor cell contribution and donor-derived B and T-lineage cells in the peripheral blood. In contrast, transplanting CLPs from the TSG-treated aging mice induced significantly higher levels of donor cell contributions as compared to those of the control aging mice, but lower than those of the young mice group (Fig. 3e). Identical trends were observed in the group with transplanted CLPs from the TSG-treated aging mice, which produced significantly higher percentages of donor cell contributions to both B and T cells in the bone marrow niche (Fig. 3f). Collectively, the data derived from these two sets of experiments manifests that the treatment of aging mice with TSG boosted the repopulation capacity of the LT-HSCs as well as the CLPs.

TSG induced significant transcription changes and promoted a quiescence signature

To investigate the potential mechanisms that govern the effects of the TSG treatment on aging HSCs, we then investigated the effects of the TSG treatment on CLP proliferation and apoptosis, as well as reactive oxygen species (ROS). The results showed that the TSG treatment did not significantly affect the percentages of BrdU-positive CLPs and Annexin V-positive CLPs in aging mice (Fig. S3a, 3b). The treatment also did not cause any significant

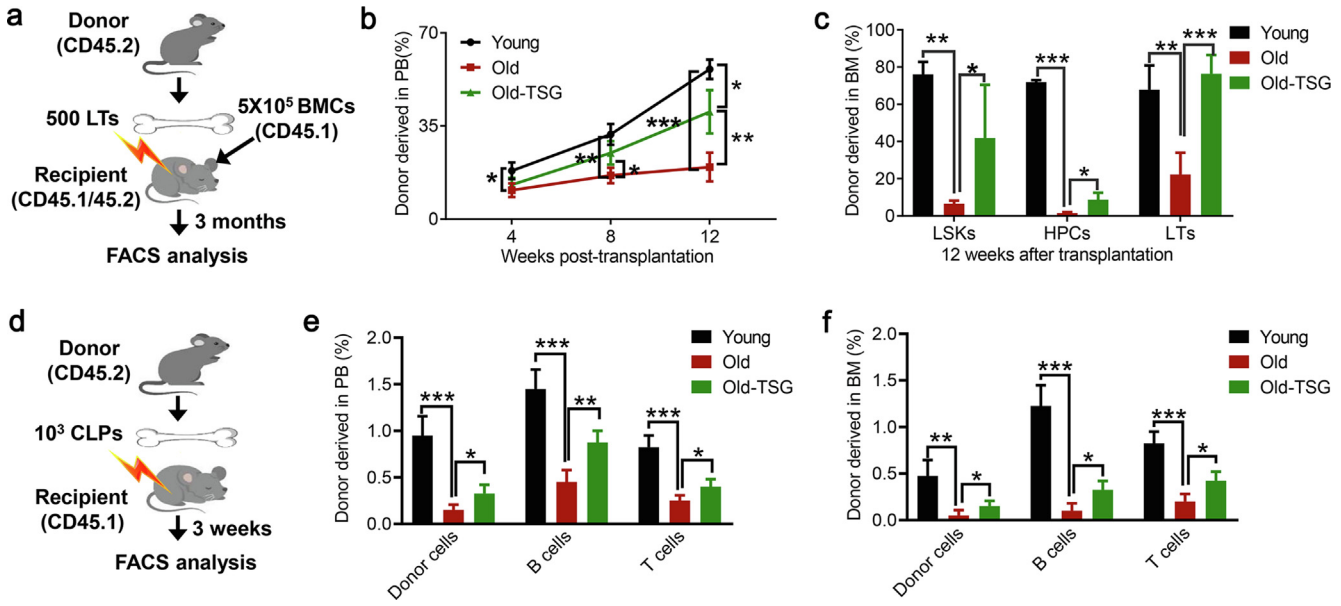

Fig. 3. Effects of TSG on the repopulation potential of HSCs of naturally aging mice. (a) The experimental scheme for the competitive transplantation experiment. Long-term hematopoietic stem cells (LTs) from donor mice were co-transplanted with bone marrow cells from competitor mice into recipient mice, which were analyzed at various time points after the competitive LTs transplantation. (b) Percentages of donor-derived cells in peripheral blood (PB) at various time points after transplantation. (c) Percentages of various subtypes of donor-derived bone marrow (BM) stem/progenitor cells at 12 weeks after transplantation (n = 5). (d) The experimental scheme for the common lymphoid progenitor (CLP) transplantation experiment. For each transplantation, 10^3 CLPs were transplanted intravenously into irradiated (4 Gy) congenic 8-week-old C57BL/6J CD45.1 mice. (e-f) Percentages of donor derived total cells, B cells, and T cells in the peripheral blood (PB) and bone marrow (BM) from recipient mice at 3 weeks after transplantation. Data is presented as mean ± S.D. (n = 5). *: $p < 0.05$; **: $p < 0.01$; ***: $p < 0.001$.

changes in the levels of intracellular ROS in LTs and CLPs compared to the control aging mice (Fig. S3c, 3d).

Aging HSCs have also been associated with certain epigenetic changes that are characterized by an altered transcriptional output with the suppression of several lymphogenic genes during the course of aging[19,20]. Thus, we also examined whether TSG could have any impact on the epigenetic profiles in the aging HSCs by conducting an analysis on the epigenetic modifications of long-term hematopoietic stem cells (LT-HSCs) from young mice, control aging mice, and TSG-treated aging mice. The results showed that the transcriptome of the HSCs from the TSG-treated aging mice exhibited a profile analogous to that of the "young" HSCs as compared to the untreated aging mice (Fig. 4a). Furthermore, gene set enrichment analysis (GSEA) and heat map analysis of 36 genes that have important roles in lymphoid lineages revealed that lymphoid-associated genes were significantly enriched in TSG-treated aging mice, which resembled the high enrichment of the genes in young mice (Fig. 4b, c). A quantitative RT-PCR (qRT–PCR) analysis of several lymphoid/myeloid-responsive genes in LTs showed that the TSG treatment substantially increased the mRNA levels in transcription factors, including Pax5, PU.1, GATA3, Ikaros (encoding genes: Zfpn1a1 and Zfpn1a3), and cytokine receptors such as IL-7 and Flk2, which are linked to the lymphoid differentiation in aging mice, even though TSG barely altered the expression of transcriptional regulators related to myeloid differentiation including E/CBPα, GATA1, and GATA2 (Fig. 4d). Recent studies have proven metabolism to be the master of HSC fate based on its most vital feature: quiescence or dormancy[21,22]. The results of the transcriptome analysis also illustrated that TSG treatment resulted in significant reductions in the expression of the oxidative phosphorylation (OXPHOS) genes, but increases in the expression levels of the quiescence-associated genes (Fig. 4e, f). These results support the contention that the TSG treatment could promote the rejuvenation of aging HSCs by reversing the aging transcriptome toward a state that is similar to that of young HSCs.

Aging HSCs are also known to be characterized by an activated metabolic state, including several modifications, such as increase in OXPHOS levels, elevation in the propensity of leaving the quiescent (G0) state to enter the cell cycle (beginning by entering the G1 phase)[14,23], etc. We found that the TSG treatment in the aging mice affected all these parameters in a positive manner. In particular, compared to the untreated control aging mice, the TSG treat-

Fig. 4. Analyses of transcriptome and metabolic status related to HSC aging. Cohorts of aging mice were treated with either vehicle (Old) or TSG (Old-TSG) for four weeks. A cohort of 8-week-old mice was included as a control for young mice (Young). (a) Clustered heatmap of the differentially expressed genes determined by RNA-seq in isolated long-term hematopoietic stem cells (LTs) from the bone marrow. Rows represent genes while columns represent LTs with 3 replicates in each group. (b) Gene set enrichment analysis (GSEA) for comparing lymphoid gene term between Young and Old as well as Old and Old-SG groups according to the results of RNA-seq. NES, normalized enrichment score; FDR, false discovery rate. (c) Heatmap for the mean expression level of genes identified as lymphoid-specific in LTs from three groups based on RNA-seq analysis. (d) Validation of lymphoid-associated and myeloid-associated genes expression by qRT-PCR in LTs isolated from the bone marrow of mice from different groups. (n = 3). (e-f) Heatmap for the mean expression level of OXPHOS related genes and HSCs quiescence related genes, respectively. (g-h) OXPHOS levels and ATP production measured by Seahorse Mito Stress analysis in the linage$^-$c-kit$^+$Sca1$^+$ hematopoietic stem cells (LSKs) isolated from bone marrow (n = 4). (i) Cell cycle distribution analysis of isolated long-term hematopoietic stem cells (LTs) from the bone marrow by FACS with Ki67 and DAPI staining (n = 4). (j) LSKs from the bone marrow were isolated to harvest total proteins for detection levels of p-AMPK (T172), total AMPK, and p-ACC (Ser79) by western blot (β-actin was used as loading control). (k) Semi-quantitative analysis of the blots was determined by Image J software (n = 3). Data is presented as mean ± S.D. *: $p < 0.05$; **: $p < 0.01$; ***: $p < 0.001$. ns: no significance.

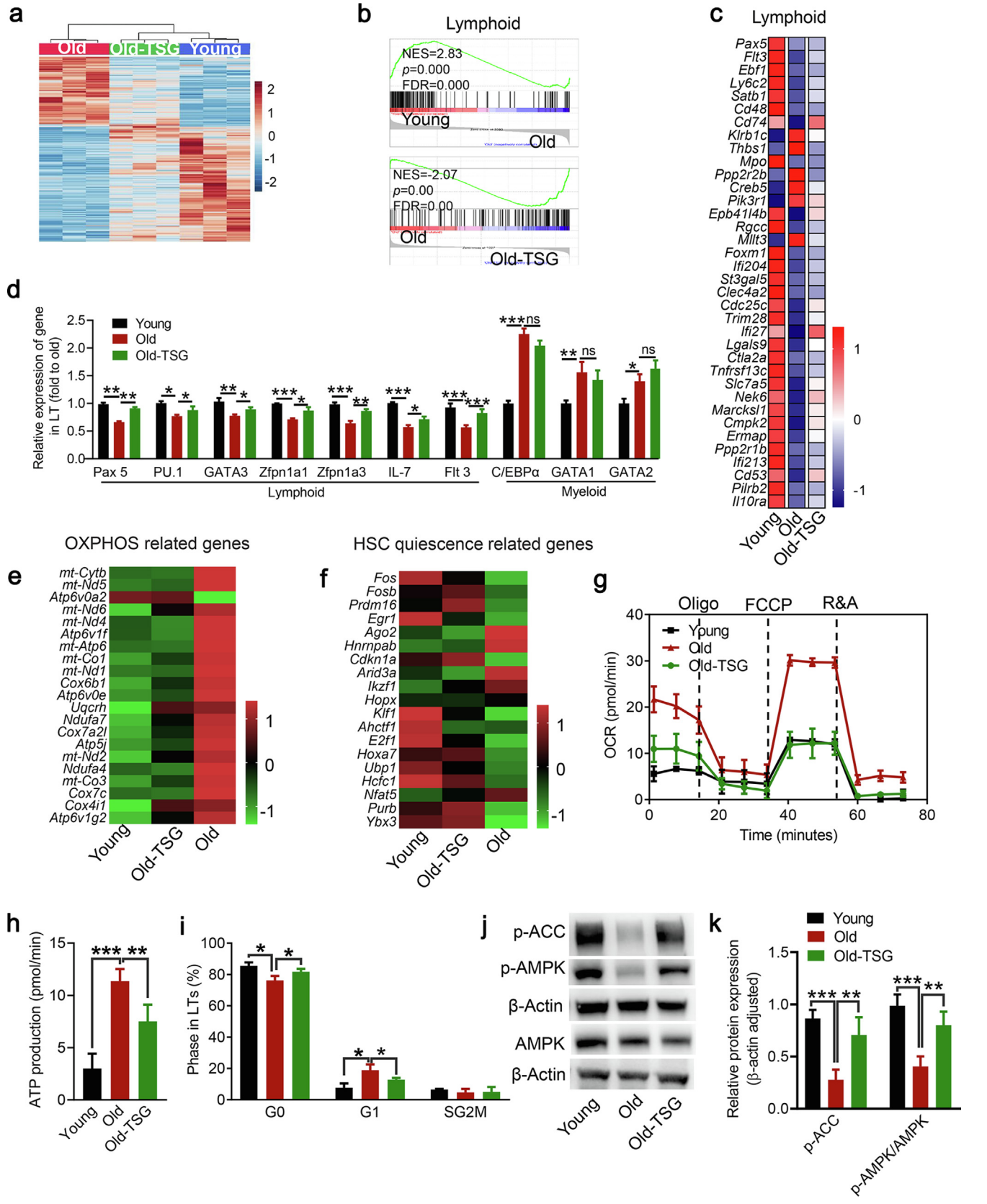
a
Old
Old-TSG
Young
2
1
0
-1
-2
b
Lymphoid
NES=2.83
p=0.000
FDR=0.000
Young
Old
NES=-2.07
p=0.00
FDR=0.00
Old
Old-TSG
c
Lymphoid
Pax5
Flt3
Ebf1
Ly6c2
Satb1
Cd48
Cd74
Klrb1c
Thbs1
Mpo
Ppp2r2b
Creb5
Pik3r1
Epb41l4b
Rgcc
Mllt3
Foxm1
Ifi204
St3gal5
Clec4a2
Cdc25c
Trim28
Ifi27
Lgals9
Ctla2a
Tnfrsf13c
Slc7a5
Nek6
Marcksl1
Cmpk2
Ermap
Ppp2r1b
Ifi213
Cd53
Pilrb2
Il10ra
1
0
-1
Young
Old
Old-TSG
d
Relative expression of gene in LT (fold to old)
Young
Old
Old-TSG
Pax 5
PU.1
GATA3
Zfpn1a1
Zfpn1a3
IL-7
Flt 3
C/EBPα
GATA1
GATA2
Lymphoid
Myeloid
e
OXPHOS related genes
mt-Cytb
mt-Nd5
Atp6v0a2
mt-Nd6
mt-Nd4
Atp6v1f
mt-Atp6
mt-Co1
mt-Nd1
Cox6b1
Atp6v0e
Ugcrh
Ndufa7
Cox7a2l
Atp5j
mt-Nd2
Ndufa4
mt-Co3
Cox7c
Cox4i1
Atp6v1g2
Young
Old-TSG
Old
f
HSC quiescence related genes
Fos
Fosb
Prdm16
Egr1
Ago2
Hnrnpab
Cdkn1a
Arid3a
Ikzf1
Hopx
Klf1
Ahctf1
E2f1
Hoxa7
Ubp1
Hcfc1
Nfat5
Purb
Ybx3
Young
Old-TSG
Old
g
Oligo
FCCP
R&A
Young
Old
Old-TSG
OCR (pmol/min)
Time (minutes)
h
ATP production (pmol/min)
Young
Old
Old-TSG
i
Phase in LTs (%)
G0
G1
SG2M
j
p-ACC
p-AMPK
β-Actin
AMPK
β-Actin
Young
Old
Old-TSG
k
Young
Old
Old-TSG
Relative protein expression (β-actin adjusted)
p-ACC
p-AMPK/AMPK

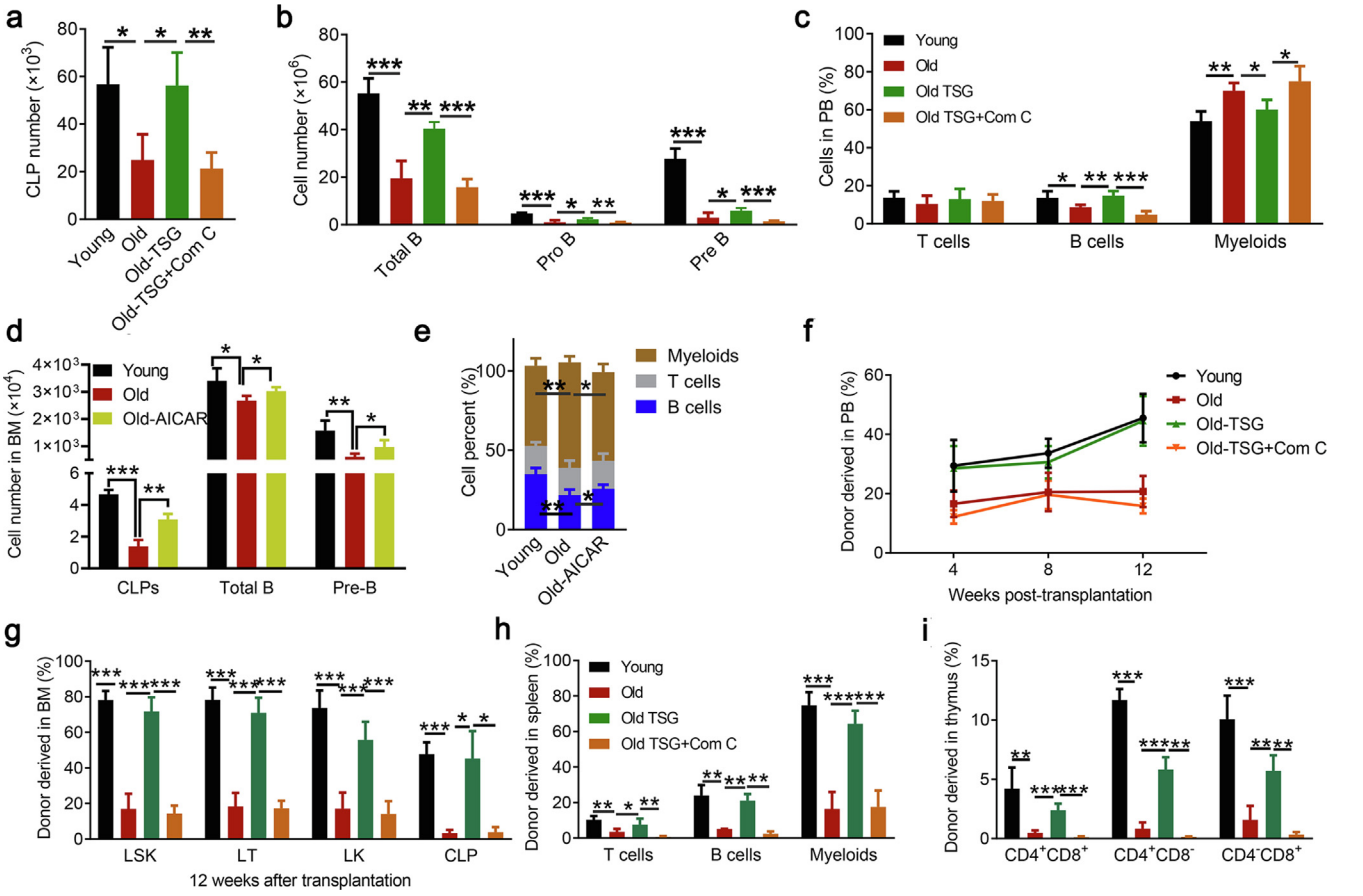

Fig. 5. Tetrahydroxy stilbene glucoside (TSG) improves hematopoietic stem cell (HSC) lymphoid differentiation and repopulation potential defects of naturally aging mice by activating AMPK. In addition to administration in mice according to the scheme shown in Fig. 1, aging mice were treated with TSG by gavage daily combined with AMP-activated protein kinase (AMPK) inhibitor compound C (Com C) by intraperitoneal injection every other day as Old-TSG + Com C group ($n = 4$). (a) Absolute numbers of CLPs in the bone marrow of different cohorts. (b) Absolute numbers of various sub-types of B cells in the bone marrow of different cohorts. (c) Quantification of the percentages of B cells, T cells, and myeloid cells in the peripheral blood. (d-e) The naturally aging mice were treated further with an activator of AMPK 5-aminoimidazole-4-carboxamide riboside (AICAR) for 60 days and analyzed. ($n = 4$). (d) The number of CLPs (the left panel in d) or the total number of B cells and pre-B cells (the right panel in d) for the 8-week-old mice (Young), the naturally aging mice treated with Vehicle (Old), and the naturally aging mice treated with AICAR (Old-AICAR) are shown. (e) Mean percentages of peripheral B, T, and myeloid cells of different cohorts. (f-i) Competitive LTs transplantation similar to experimental design of Fig. 2a (5 recipients per group). (f) Percentage of donor-derived cells in the peripheral blood of recipient mice at 4, 8, and 12 weeks after competitive LT transplants. (g) Percentages of various subtypes of donor-derived bone marrow stem/progenitor cells at 12 weeks post competitive LT transplantation. (h) Spleen analyzed for percentages of donor-derived cells at 12 weeks after transplantation. (i) Thymus analyzed for percentages of donor-derived cells at 12 weeks after transplantation. Data is expressed as mean ± SD. $^{*}P < 0.05$, $^{**}P < 0.01$, $^{***}P < 0.001$ compared between the indicated groups.

ment resulted in a shift in oxygen consumption rates (OCR) profile from the aging phenotype toward a pattern that are closer to that of the young HSCs (Fig. 4g). In addition, the TSG treatment also led to a significant suppression of the ATP utilization (Fig. 4h), a substantial increase in the fraction of G0 sub-population, along with a significant reduction in the fraction of G1 sub-population (Fig. 4i), indicative of a more quiescent state. Considering AMPK is a critical energy sensor other than being one of the master regulators of energy metabolism, we investigated the possible effect of the TSG treatment on the AMPK pathway. The results showed that the level of AMPK-T172 phosphorylation (p-AMPK-T172) and its substrate phosphorylation of acetyl-CoA carboxylase (p-ACC-Ser79) were elevated in the extract of LSKs from the TSG-treated aging mice. Yet, the total AMPK hardly suffered a change in protein levels (Fig. 4j-k). Overall, this data suggests that TSG could suppress the metabolism of aging HSCs, promote the activation of the AMPK pathway and a change toward a state of quiescence.

The effect of TSG in rejuvenating aging HSCs is dependent on the AMPK pathway

To further validate the rejuvenation nature of AMPK in TSG for HSC aging, we utilized specific AMPK inhibitor compound C (Com C) to inhibit the activation of AMPK to explore the effects of TSG on HSC aging in mice. Notably, Com C considerably blocked the protective effects of TSG on the number of CLPs and downstream B cells in the bone marrow, as well as the proportion of B cells in the peripheral blood of aging mice (Fig. 5a-c). Furthermore, we also investigated whether 5-aminoimidazole-4-carboxamide riboside (AICAR), an activator for AMPK, has a potency for rejuvenating aging cells. As expected, we found that AICAR treatment could raise the numbers of CLPs and/or the total number of B and pre-B cells in the bone marrow, as well as redress the imbalance in the peripheral blood as an increase in the percentage of B cells and decrease in the percentage of myeloid cells for the naturally aging mice in a similar manner (Fig. 5d-e). To determine whether repopulation

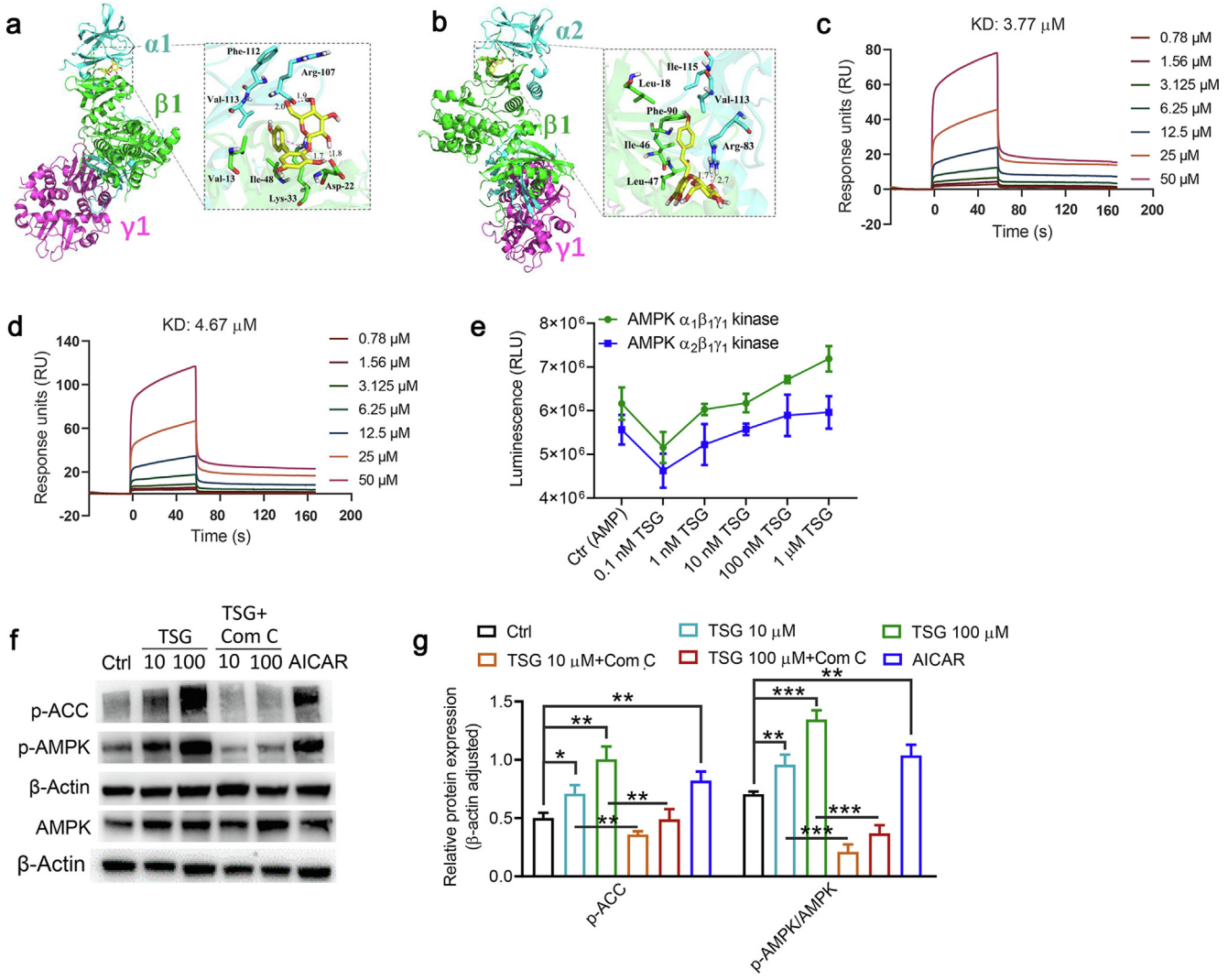

Fig. 6. Tetrahydroxy stilbene glucoside (TSG) interacts with AMPK in vitro. (a-b) Molecular docking study of the binding affinity of TSG to AMPKα1β1γ1 and AMPKα2β1γ1 crystal structures. (c-d) SPR analyses of the interaction of TSG with AMPKα1β1γ1 and AMPKα2β1γ1. (e) Effect of TSG on the kinase activity of AMPK in a cell-free system. AMPKα1β1γ1 and AMPKα2β1γ1 kinase enzyme system treated with AMP (positive control) or different concentration of TSG were detected using ADP-GloTM kinase assay reagents for the luminescent signal (n = 4). (f) Representative western blot analysis of p-AMPK (T172), total AMPK, p-ACC (Ser79) and β-actin in senescent IMR-90 cells treated with vehicle, different concentrations of TSG (10 and 100 μM), AMPK inhibitor Comp C (10 μM) combined with TSG or AMPK activator AICAR (0.5 mM) for 48 h. (g) Semi-quantitative analysis of the blots was determined by Image J software (n = 3). Data is presented as mean ± S.D. *: $p < 0.05$; **: $p < 0.01$; ***: $p < 0.001$.

potential of LTs ameliorated by TSG depended on AMPK, we performed the competitive transplantation experiment. The results of the experiment showed that the degree of donor chimerism in the peripheral blood decreased dramatically in TSG + Com C co-treated aging mice compared to that of the mice treated with TSG alone (Fig. 5f). Furthermore, the co-treatment with Com C also led to a significant decrease in the percentage of donor-derived HPSCs in the bone marrow of TSG-treated aging mice at twelve weeks after the transplantation Fig. 5g). The treatment, however, did not lead to any significant changes in the degrees of donor-derived chimerism in spleen and thymus (Fig. 5h, i). Overall, these results suggest that TSG could effectively enhance HSC function and lymphoid differentiation mainly through the activation of AMPK.

TSG could physically interact with AMPK in vitro

To further examine the molecular mechanisms of TSG for HSC aging via activating AMPK, we applied drug-protein molecular interaction analyses. Molecular docking was applied to investigate the binding modes of TSG with AMPKα1β1γ1 (PDB: 6C9F) and AMPKα2β1γ1 (PDB: 6B1U). The results showed that TSG could bind to the kinase domain of the AMPKα1β1γ1 and AMPKα2β1γ1 proteins with relative high docking-scores of −6.45 and −5.83, respectively (Fig. 6a, b). Moreover, the results of a surface plasmon resonance (SPR) revealed the association and dissociation of TSG with immobilized AMPKα1β1γ1 and AMPKα2β1γ1. As shown in Fig. 6c and 6d, TSG could bind to AMPKα1β1γ1 with a higher affinity (KD = 3.77 μM) than AMPKα2β1γ1 (KD = 4.67 μM). Additionally, ADPGlo™ kinase assay was performed to measure luminescence-based AMPK activity. The results showed that AMPKα1β1γ1 and AMPKα2β1γ1 were activated by the TSG at various concentrations ranging from 0.1 nm to 1 μM (AMP was used as a positive control) (Fig. 6e). Furthermore, we studied the effects of the TSG in AMPK activity using specific AMPK inhibitor Com C and AMPK agonist AICAR on senescent human fibroblasts (IMR-90), since this cell line has been widely used to concentrate on replicative prompted senescence in culture. Using the western blotting, we found that AMPKα T172 and acetyl-CoA carboxylase (ACC) phosphorylation levels were ultimately increased in a dose

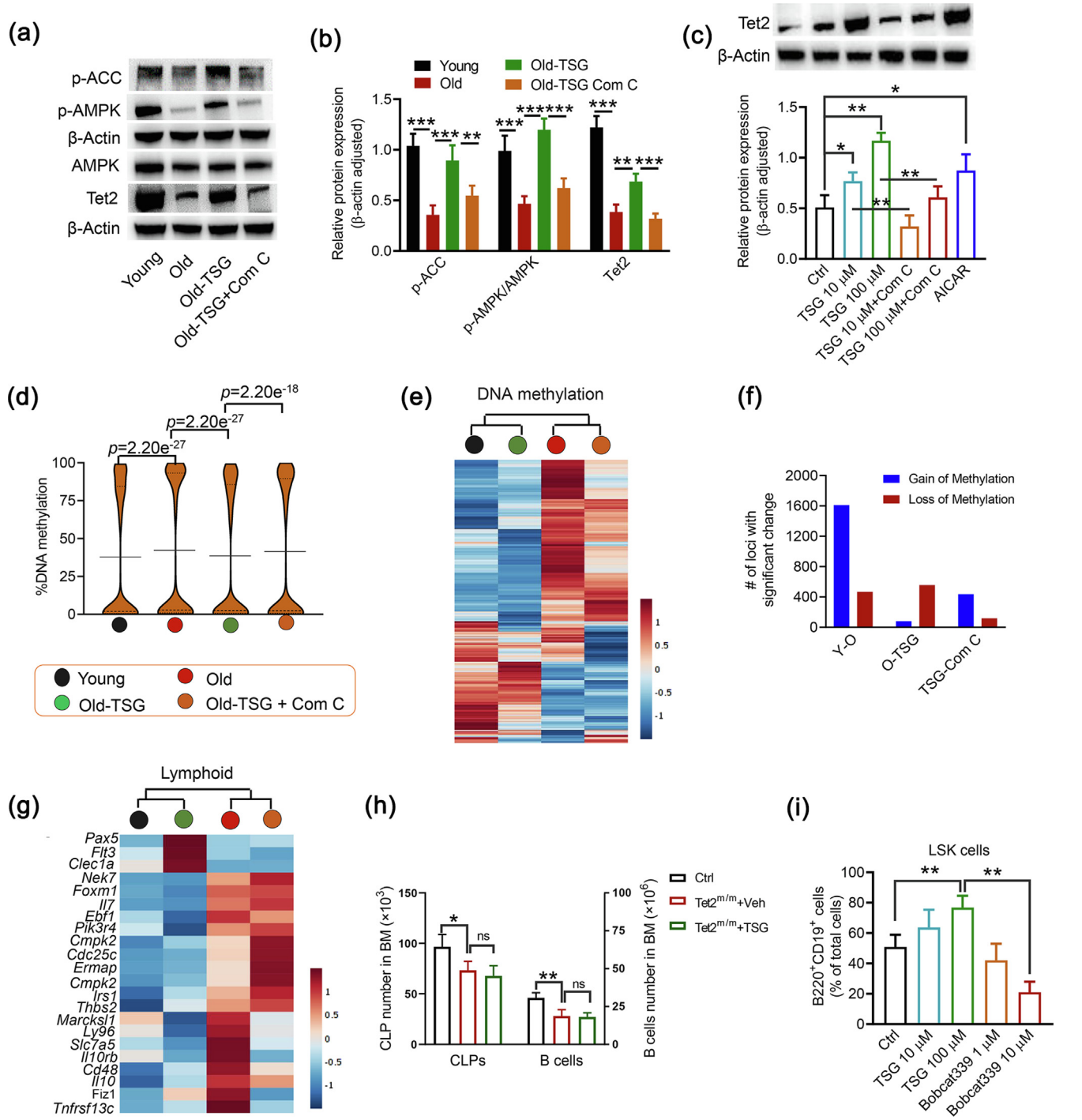

Fig. 7. Tetrahydroxy stilbene glucoside (TSG) affects the fate of hematopoietic stem cells (HSCs) through *Tet2*-mediated epigenetic regulation. (a) Linage⁻c-kit⁺Sca1⁺ hematopoietic stem cells (LSKs) from the bone marrow of different cohorts according to the experimental procedure of Fig. 5 were isolated to harvest total proteins for detection levels of p-AMPK (T172), total AMPK, p-ACC (Ser79), and Tet2 by western blot (β-actin was used as loading control). (b) Semi-quantitative analysis of the blots was determined by Image J software (n = 4). (c) Representative western blot and semi-quantitative analysis of Tet2 and β-actin in senescent IMR-90 cells treated with vehicle, different concentrations of TSG (10 and 100 μM), AMPK inhibitor Comp C (10 μM) combined with TSG or AMPK activator AICAR (0.5 mM) for 48 h (n = 3). (d-g) Long-term hematopoietic stem cells (LTs) were isolated from the bone marrow for the DNA methylation analysis. (d) Bean plots of global DNA methylation of LTs from Young, Old, Old-TSG, and Old-TSG + Com C groups. (e) Hierarchical clustering of representative 100 kb tiles of DNA methylation data of LTs from mice of four groups. (f) Number of 1 kb tiles with significant methylation differences in pairwise comparisons between LTs isolated from different groups. Total comparisons with sufficient DNA methylation data from three populations, Y-O: Young LTs to Old LTs, O-TSG: Old LTs to Old-TSG LTs, Old-TSG LTs to Old-TSG + Com C LTs. (g) Heat map of DNA methylation levels of lymphoid-specific genes in LTs. Blue denotes low methylation levels and red denotes high expression. (h) 40-week-old *Tet2* mutant mice were treated with vehicle or TSG by gavage once a day continuously for 60 days, a cohort of 40-week-old littermate control mice were treated with vehicle (Ctrl). The number of CLPs (the left panel in h) and the total number of B cells (the right panel in h) in the bone marrow of the mice are shown. (i) Lymphoid differentiation potential of LSKs from the bone marrow of 8-week-old mice. 1,000 sorted LSKs were seeded onto OP9 stromal cells supplemented with cytokines needed for lymphoid differentiation and numbers of B220 and CD19 double-positive cells were calculated at the indicated intervals by FACS ($n = 4$). Error bars represent mean ± SD. $^{**}P < 0.01$, $^{***}P < 0.001$ compared between the indicated groups. (For interpretation of the references to colour in this figure legend, the reader is referred to the web version of this article.)

dependent manner after TSG treatment, which were even a little better than the AICAR. Simultaneously, interference with Com C with TSG, phosphorylation of AMPK and ACC were dramatically decreased compared to the TSG treatment (Fig. 6f, g). Taken together, these results indicate that TSG could promote AMPK activation through a direct interaction with the AMPK enzyme.

TSG could reverse methylation profile of aging HSCs through AMPK-Tet2 axis

The epigenetic alterations are closely linked to the phenotypic and functional changes that have been documented for HSCs [24,25]. Ten-Eleven-Translocation 2 (Tet2), deemed as a crucial epigenetic regulator, is instrumental in homeostasis and differentiation of HSCs[26]. Previous studies have shown that AMPK activation is critical to maintain the Tet2 stability[27,28]. Thus, we then also analyzed the effects of TSG on the activation of AMPK and the expression of Tet2 (Fig. 7a, b). In cell culture, we also found that TSG effectively increased the level of Tet2, but the effect was significant diminished by co-treatment with Com C (Fig. 7c). Since Tet2 contributed to the epigenetic status of DNA by oxidizing 5-methylcytosine (5mC) to 5-hydroxymethylcytosine (5hmC) to promote gene expression, we then assessed genomic-wide DNA methylation status of LTs using the reduced representation bisulfite sequencing (RRBS) analysis. The results showed that LTs from aging mice exhibited a significant increase in the level of global DNA methylation, specifically at a level of 40.16 % compared to 37.36 % of those from the young mice. The TSG-treatment in aging mice resulted in a significant decline in the level of DNA methylation, to a level that is very similar to that of the young mice. Furthermore, this effect was diminished with the co-treatment of Com C (Fig. 7d). Hierarchical clustering analysis of the methylation profiles revealed that the LTs from the four groups fell into two categories, with the young and the old-TSG groups clustered together, while the old and the old-TSG + Com C groups fell in the same cluster (Fig. 7e). A pairwise comparison analysis revealed a few thousand loci that exhibited either a gain or a loss of DNA methylation during HSC ontogeny (Fig. 7f). Specifically, the methylation levels of lymphoid-regulated genes of LTs showed a decrease in TSG-treated aging mice, but were elevated in TSG and Com C co-treated aging mice (Fig. 7g). This data suggests that Tet2 could play a key role in the effect of TSG on DNA methylation in aging HSCs. Indeed, TSG treatment did not lead to a significant increase in the absolute number of CLPs and B cells in *Tet2* mutant mice (Fig. 7h). We then also carried out an in vitro LSKs co-culture assay to investigate the effect of TSG on lymphopoiesis. The results showed that TSG treatment led to a significant increase in the potential of lymphopoiesis of bone marrow LSKs from 8-week-old mice, and that this effect was attenuated by Tet2 inhibitor Bobcat339 (Fig. 7i). In aggregate, these data support a model that Tet2 functions as a downstream effector of AMPK activation to promote the lymphopoiesis potential of HSCs and that TSG could promote lymphopoiesis by affecting this AMPK-Tet2 axis. All these experiments were repeated at least three times and the results were highly reproducible.

Discussion

The demonstration of the reversible nature of HSC aging has raised the prospect of rejuvenating aging HSCs through specific interventions, including pharmacological drug treatments[6]. Yet, the development of such drugs through the conventional modern drug development paradigm is likely to be a challenging task with major commitments of resources and time. In this context, the claim of the existence of efficacious anti-aging TCM formulas presents a unique alternative path for addressing this challenge. TCM products are approved drugs in some regions/countries, particularly in China, and have been known for their exceptional safety attributes. Moreover, the major molecular entities of the key components of these formulas have been extensively documented and often times the candidate active compounds have been purified. Yet, a major issue is that the claimed therapeutic effects are often not proven by the results of proper modern randomized clinical trials. Thus, we have argued that with respect to the formulas that have been claimed to have potent anti-aging potentials, the validation of the efficacy would be a great start to the rapid expansion of the use of these drugs and/or a great incentive for promoting the development of the relevant compounds into anti-aging drugs through the modern drug development path.

In this study, we have demonstrated that the system with the use of both the TBI mice and naturally aging mice is a very effective and a reliable system for assessing whether a compound is effective in rejuvenating aging HSCs. With the system, we have succeeded in identifying TSG, a compound isolated from the acclaimed anti-aging TCM component ‘‘Heshouwu”, as an effective agent for rejuvenating aging HSCs in aging mice. This has therefore provided the proof-of-concept of the system for assessing the potential of individual substances in rejuvenating aging HSCs. In addition, we have also showed that TSG promoted the lymphopoiesis tendency as well as the potential of repopulation both in naturally aging mice and TBI-induced aging mice by activating AMPK-Tet2 axis. Such an exercise has demonstrated the power of the system for interrogating the mechanisms of rejuvenating aging HSCs for a substance of interest, which in the context of a screening endeavor, would provide additional assurance for the efficacy of the candidate identified.

Researches have proved both intrinsic and extrinsic mechanisms are involved in regulating aging HSCs function or lymphoid differentiation defect[29]. Age-related changes in the bone marrow niche microenvironment influence these decline generally as oxidative stress, hormone and inflammation[30]. Intriguingly, it has also been reported that TSG could exert a significant anti-degenerative effect in neuronal cells by modulating the Nrf2-HO-1 pathway to maintain the redox homeostasis[31–34], raising the prospect that TSG could work as a defense in oxidative stress-driven degenerative diseases or perhaps others. Stem cells also need to be protected from high oxidative stress to avoid stem cell exhaustion and insufficient host immunity. However, TSG even with powerful oxidation resistance had not reduced high ROS levels of HSCs in ageing mice, which authentically needs further in-depth study to search for the underlying causes or detailed exploration. Another recent study demonstrated that sex steroid ablation (SSA) induced hematopoietic and lymphoid recovery by enhancing self-renewal of old HSCs, whereas the function of CLPs does not change, but TSG remarkably strengthened the function of old HSCs as well as CLPs[35]. Inflammation may play an important role in HSCs ageing, but a recent study shows that reducing the level of inflammation does not affect the rejuvenation of lymphocyte development[36]. All above statements suggest that the pharmacological role of TSG against HSCs aging is likely extrinsic context independent.

Metabolism and epigenetics intertwine in a very complex manner and interplay between themselves to influence the aging process. Inspired by the view of metabolic reprogramming with epigenetic modifications for the control of HSC fate in aged mice, we found that the activation of AMPK was instrumental in maintaining HSC function and lymphoid differentiation, and conducive effects of TSG on aging HSCs are AMPK-dependent through the supplementation of AMPK inhibitor Com C or AMPK activator AICAR**.** DNA methylation, termed the ‘epigenetic clock’ is used for predicting chronological age in a variety of tissues, and is regulated

by DNA methyltransferases and Tet enzymes, and certified to underlie HSC aging[24,37]. Herein, we observed that the TSG treatment altered DNA methylation profile of aging HSCs, and even reverted them to a youthful level, and it was AMPK-dependent to a great extent, as Com C effectively evaded changes caused by TSG in methylation profile. AMPK-mediated phosphorylation stabilizes Tet2 for tumor suppression by an epigenetic pathway[27], and *Tet2* mutant mice exhibits impairments of lymphopoiesis [13], which prompted us to link TSG-activated AMPK to Tet2 for probing this possibility in selective elevation of lymphoid gene expression. As expected, activation of AMPK regulated by TSG coincided with the increased protein level of *Tet2* in aging mice, while the TSG treatment in the *Tet2* mutant mice failed to restore the CLP counts as compared to the vehicle-treated *Tet2* mutant mice, which were further verified with the treatment of Tet2 inhibitor Bobcat339 in inhibiting lymphoid differentiation potential using LSKs-OP9 co-culture assay in vitro. Our study demonstrated that TSG operated anti-aging effects through the AMPK-Tet2 axis *in vivo*, and fitness of AMPK-Tet2 may, thus, signify the therapeutic targets for rejuvenating aging HSCs.

Like many TCM components, "Heshouwu" has been used for a long time in China as either a medicinal herb or a nutritional supplement. It has proven safe when the proper usage guidelines are carefully followed[38]. Yet, this herb has also been known for its potential of causing significant adverse effects when misused [39]. It is worth noting that it has been reported that the *trans*-isomer is the effective compound whereas its *cis*-isomer is not only ineffective but could cause harmful effects[40,41]. In this context, the demonstration of the efficacy of TSG in rejuvenating aging HSCs has validated the claim of anti-aging effect of "Heshouwu" and likely will promote the use of this herb. Together, this new information could greatly enhance the safe use of this herb and/or TSG, and promote the development of TSG-based drugs through the modern drug development paradigm. In this regard, it is noted that TSG is highly soluble in water and could have desirable attributes for drug development.

In summary, we have successfully identified TSG as a potent agent for rejuvenating aging HSCs with predilection for lymphoid differentiation in mice, and activation of AMPK-Tet2 axis may thus represent therapeutic targets for preventing HSCs aging. Together, our data have provided the proof-of-concept of the efficacy of the systematic strategy for evaluating the potential of individual agents for rejuvenating aging HSCs. The research mode is compatible with most conventional drug development programs and hence, should prove invaluable for the development of drugs for delaying and/or reversing impairments caused by aging of HSCs in humans. Also, the demonstration that TSG exhibited excellent efficacy in rejuvenating aging HSCs in mice could have a direct impact in accelerating the clinical translation of this compound as well as the TCM component from which it was isolated.

Compliance with Ethics Requirements

All mice tests were carried out in compliance with protocols authorized by the Animal Care and Ethics Committee at the Fifth Medical Centre, Chinese PLA (People's Liberation Army) General Hospital, and the ethical authorization number was IACUC-2020-0048 approved at July 12, 2020.

Declaration of competing interest

The authors declare that they have no known competing financial interests or personal relationships that could have appeared to influence the work reported in this paper.

Acknowledgments

We are grateful to Drs. Shaorong Gao and Jiayu Chen from the Tongji University for providing the *Tet2* mutant mice; Drs. Yezhang Zhu, Miao Shi and Li Shen from Zhejiang University for the DNA methylation analysis. This work was supported by the Beijing Natural Science Foundation (JQ21026), CMU Talent Project (1220090104), National Key R&D Program of China (2021YFA1100090), the National Natural Science Foundation of China (81803537, 82274121, 82074112), Innovative Team Program of Guangzhou Regenerative Medicine and Health Guangdong Laboratory (2018GZR110103002), the project of Key Laboratory of Endemic and Ethnic Diseases, Ministry of Education, Guizhou Medical University (FZSW-2021-004).

Appendix A. Supplementary data

Supplementary data to this article can be found online at https://doi.org/10.1016/j.jare.2024.04.027.

References

[1] Kasbekar M, Mitchell CA, Proven MA, Passegué E. Hematopoietic stem cells through the ages: a lifetime of adaptation to organismal demands. Cell Stem Cell 2023;30:1403–20.
[2] Pang WW, Schrier SL, Weissman IL. Age-associated changes in human hematopoietic stem cells. Semin Hematol 2017;54:39–42.
[3] Geiger H, de Haan G, Florian MC. The ageing haematopoietic stem cell compartment. Nat Rev Immunol 2013;13:376–89.
[4] de Haan G, Lazare SS. Aging of hematopoietic stem cells. Blood 2018;131:479–87.
[5] Broxmeyer HE, Liu Y, Kapur R, Orschell CM, Aljoufi A, Ropa JP, et al. Fate of hematopoiesis during aging. what do we really know, and what are its implications? Stem Cell Rev Rep 2020;16:1020–48.
[6] Li X, Zeng X, Xu Y, Wang B, Zhao Y, Lai X, et al. Mechanisms and rejuvenation strategies for aged hematopoietic stem cells. J Hematol Oncol 2020;13:31.
[7] Mahmoudi S, Xu L, Brunet A. Turning back time with emerging rejuvenation strategies. Nat Cell Biol 2019;21:32–43.
[8] Jiang Z, Wang W, Guo C. Tetrahydroxy stilbene glucoside ameliorates H2O2-induced human brain microvascular endothelial cell dysfunction in vitro by inhibiting oxidative stress and inflammatory responses. Mol Med Rep 2017;16:5219–24.
[9] Zou Y, Kong M. Tetrahydroxy stilbene glucoside alleviates palmitic acid-induced inflammation and apoptosis in cardiomyocytes by regulating miR-129-3p/Smad3 signaling. Cell Mol Biol Lett 2019;24:5.
[10] Zhang J, Chen X, Chen B, Tong L, Zhang Y. Tetrahydroxy stilbene glucoside protected against diabetes-induced osteoporosis in mice with streptozotocin-induced hyperglycemia. Phytotherapy research : PTR 2019;33:442–51.
[11] Gao D, Chen C, Huang R, Yang CC, Miao BB, Li L, et al. Tetrahydroxy stilbene glucoside ameliorates cognitive impairments and pathology in APP/PS1 transgenic mice. Curr Med Sci 2021;41:279–86.
[12] Miao BB, Gao D, Hao JP, Li YL, Li L, Wang JB, et al. Tetrahydroxy stilbene glucoside alters neurogenesis and neuroinflammation to ameliorate radiation-associated cognitive disability via AMPK/Tet2. Int Immunopharmacol 2022;110:108928.
[13] Ito K, Lee J, Chrysanthou S, Zhao Y, Josephs K, Sato H, et al. Non-catalytic roles of Tet2 are essential to regulate hematopoietic stem and progenitor cell homeostasis. Cell Rep 2019;28. 2480-90.e4.
[14] Ho TT, Warr MR, Adelman ER, Lansinger OM, Flach J, Verovskaya EV, et al. Autophagy maintains the metabolism and function of young and old stem cells. Nature 2017;543:205–10.
[15] Chang J, Wang Y, Shao L, Laberge RM, Demaria M, Campisi J, et al. Clearance of senescent cells by ABT263 rejuvenates aged hematopoietic stem cells in mice. Nat Med 2016;22:78–83.
[16] Wang Y, Schulte BA, LaRue AC, Ogawa M, Zhou D. Total body irradiation selectively induces murine hematopoietic stem cell senescence. Blood 2006;107:358–66.
[17] Geiger H, Rudolph KL. Aging in the lympho-hematopoietic stem cell compartment. Trends Immunol 2009;30:360–5.
[18] Akunuru S, Geiger H. Aging, Clonality, and Rejuvenation of Hematopoietic Stem Cells. Trends Mol Med 2016;22:701–12.
[19] Sun D, Luo M, Jeong M, Rodriguez B, Xia Z, Hannah R, et al. Epigenomic profiling of young and aged HSCs reveals concerted changes during aging that reinforce self-renewal. Cell Stem Cell 2014;14:673–88.
[20] Farlik M, Halbritter F, Müller F, Choudry FA, Ebert P, Klughammer J, et al. DNA Methylation dynamics of human hematopoietic stem cell differentiation. Cell Stem Cell 2016;19:808–22.

[21] Girotra M, Chiang YH, Charmoy M, Ginefra P, Hope HC, Bataclan C, et al. Induction of mitochondrial recycling reverts age-associated decline of the hematopoietic and immune systems. Nat Aging 2023;3:1057–66.
[22] Khorraminejad-Shirazi M, Farahmandnia M, Kardeh B, Estedlal A, Kardeh S, Monabati A. Aging and stem cell therapy: AMPK as an applicable pharmacological target for rejuvenation of aged stem cells and achieving higher efficacy in stem cell therapy. Hematol Oncol Stem Cell Ther 2018;11:189–94.
[23] Treichel S, Filippi MD. Linking cell cycle to hematopoietic stem cell fate decisions. Front Cell Dev Biol 2023;11:1231735.
[24] Liu R, Zhao E, Yu H, Yuan C, Abbas MN, Cui H. Methylation across the central dogma in health and diseases: new therapeutic strategies. Signal Transduct Target Ther 2023;8:310.
[25] Aoyama K, Itokawa N, Oshima M, Iwama A. Epigenetic Memories in Hematopoietic Stem and Progenitor Cells. Cells 2022;11:2187.
[26] Hong T, Li J, Guo L, Cavalier M, Wang T, Dou Y, et al. TET2 modulates spatial relocalization of heterochromatin in aged hematopoietic stem and progenitor cells. Nat Aging 2023;3:1387–400.
[27] Wu D, Hu D, Chen H, Shi G, Fetahu IS, Wu F, et al. Glucose-regulated phosphorylation of TET2 by AMPK reveals a pathway linking diabetes to cancer. Nature 2018;559:637–41.
[28] Fiedler EC, Shaw RJ. AMPK Regulates the Epigenome through Phosphorylation of TET2. Cell Metab 2018;28:534–6.
[29] Zhang L, Mack R, Breslin P, Zhang J. Molecular and cellular mechanisms of aging in hematopoietic stem cells and their niches. J Hematol Oncol 2020;13:157.
[30] Morrison SJ, Scadden DT. The bone marrow niche for haematopoietic stem cells. Nature 2014;505:327–34.
[31] Calabrese V, Cornelius C, Dinkova-Kostova AT, Calabrese EJ, Mattson MP. Cellular stress responses, the hormesis paradigm, and vitagenes: novel targets for therapeutic intervention in neurodegenerative disorders. Antioxid Redox Signal 2010;13:1763–811.
[32] Calabrese V, Giordano J, Signorile A, Laura Ontario M, Castorina S, De Pasquale C, et al. Major pathogenic mechanisms in vascular dementia: Roles of cellular stress response and hormesis in neuroprotection. J Neurosci Res 2016;94:1588–603.
[33] Concetta Scuto M, Mancuso C, Tomasello B, Laura Ontario M, Cavallaro A, Frasca F, et al. Curcumin, Hormesis and the Nervous System. Nutrients 2019; 11
[34] Jiao C, Gao F, Ou L, Yu J, Li M, Wei P, et al. Tetrahydroxy stilbene glycoside (TSG) antagonizes Aβ-induced hippocampal neuron injury by suppressing mitochondrial dysfunction via Nrf2-dependent HO-1 pathway. Biomedicine & pharmacotherapy = Biomedecine & pharmacotherapie 2017;96:222–8.
[35] Khong DM, Dudakov JA, Hammett MV, Jurblum MI, Khong SM, Goldberg GL, et al. Enhanced hematopoietic stem cell function mediates immune regeneration following sex steroid blockade. Stem Cell Rep 2015;4:445–58.
[36] Dorshkind K, Höfer T, Montecino-Rodriguez E, Pioli PD, Rodewald HR. Do haematopoietic stem cells age? Nat Rev Immunol 2020;20:196–202.
[37] Svendsen AF, de Haan G. Is the philosopher's stone to rejuvenate blood stem cells an epigenetic regulator? Nat Aging 2022;2:980–1.
[38] Lin L, Ni B, Lin H, Zhang M, Li X, Yin X, et al. Traditional usages, botany, phytochemistry, pharmacology and toxicology of Polygonum multiflorum Thunb.: a review. J Ethnopharmacol 2015;159:158–83.
[39] Liu Y, Wang W, Sun M, Ma B, Pang L, Du Y, et al. Polygonum multiflorum-induced liver injury: clinical characteristics, risk factors, material basis, action mechanism and current challenges. Front Pharmacol 2019;10:1467.
[40] Meng YK, Li CY, Li RY, He LZ, Cui HR, Yin P, et al. Cis-stilbene glucoside in Polygonum multiflorum induces immunological idiosyncratic hepatotoxicity in LPS-treated rats by suppressing PPAR-γ. Acta Pharmacol Sin 2017;38:1340–52.
[41] Li C, Niu M, Bai Z, Zhang C, Zhao Y, Li R, et al. Screening for main components associated with the idiosyncratic hepatotoxicity of a tonic herb. Polygonum multiflorum Front Med 2017;11:253–65.